A Fast Newton-Raphson Method in Stochastic Linearization

Thomas Canor[1], Nicolas Blaise[1], Vincent Denoël[1]
[1]Structural Engineering Division, University of Liège, Chemin des Chevreuils, B52/3, 4000 Liège, Belgium
email: t.canor@ulg.ac.be, n.blaise@ulg.ac.be, v.denoel@ulg.ac.be

ABSTRACT: Owing to its accessible implementation and rapidity, the equivalent linearization has become a common probabilistic approach for the analysis of large-dimension nonlinear structures, as encountered in earthquake and wind engineering. It consists in replacing the nonlinear system by an equivalent linear one, by tuning the parameters of the equivalent system, in order to minimize some discrepancy error. Consequently classical analysis tools such as the spectral analysis may be reconditioned to approximate the solution of structures with slight to moderate nonlinearities. The tuning of the equivalent parameters requires the solution of a set of nonlinear algebraic equations involving integrals. It is typically performed with the fixed-point algorithm, which is known to behave poorly in terms of convergence. We therefore advocate for the use and implementation of a Newton-Raphson approach, which behaves much better, even in its dishonest formulation. Unfortunately, this latter option requires the costly construction of a Jacobian matrix. In the approach described in this paper, this issue is answered by introducing a series expansion method that provides a fast and accurate estimation of the residual function (whose solution provides the equivalent parameters) and a fast and approximate estimation of the Jacobian matrix. An illustration demonstrate the good accuracy obtained with the proposed method.

KEY WORDS: modal coupling; nonlinear; series expansion; asymptotic expansion.

1 INTRODUCTION

In many engineering matters, structures are subject to random excitations. Probabilistic theories aim at describing their random structural responses by means of statistical characteristics such as probability density functions or cumulants [1,2]. These theories are well established and readily applicable for classical problems like the stochastic analysis of linear deterministic systems [3], but are scarcely applicable in a much wider sense like for instance in the presence of a nonlinear structural behavior. Conversely the Monte-Carlo approach is compatible with the widest range of applications such as those involving nonlinearities, large size structures or non markovian loading processes. The numerical implementation of a simulation technique has however a certain cost, especially when it comes to analyzing large-dimension structures.

At a design stage, approximate probabilistic methods are thereby preferred. Among them, the equivalent linearization is frequently applied for the analysis of large-dimension nonlinear structures, as encountered in earthquake and wind engineering. In fact, it is all the more well adapted to these fields that these loadings, wind and earthquakes, are or might be provided by means of a spectral representation. The main idea of the equivalent linearization consists in replacing the nonlinear system by an equivalent linear one, by tuning the parameters of the equivalent system in order to minimize a mean-square discrepancy.

The Gaussian equivalent linearization expresses the properties of an equivalent linear system in terms of the covariance matrix of the response of the system. Even though the system has been linearized, the set of equations to calculate the covariance matrix is nonlinear. The computational effort in this method pertains to the resolution of this (possibly large) set of nonlinear algebraic equations involving integrals. The format of this set of equation is actually well adapted to the use of a fixed-point algorithm which is recommended in dedicated literature [4]. We presume it is also of standard application in common practice, although this kind of detail is seldom reported. The use of this low-order and sometimes badly conditioned algorithm is surprising at first glance. It is seemingly justified by the *a priori* expensive cost of the Jacobian of the problem that would allow for second-order algorithms such as the Newton algorithm.

Thanks to a perturbation approach, which was formerly investigated by the authors in similar applications [5, 6], the stochastic linearization of a large scale structure is reformulated in a novel framework which opens the possible implementation of a second-order method, at few extra costs compared to the standard application. These developments are presented in this paper, together with some illustrative examples demonstrating the benefits of the approach.

2 MATHEMATICAL SETTING

2.1 Stochastic Linearization in a Reduced Basis

The equation of motion of an *n*-DOF nonlinear system reads

$$\mathbf{M}\ddot{\mathbf{y}} + \mathbf{C}\dot{\mathbf{y}} + \mathbf{K}\mathbf{y} + \mathbf{g}(\mathbf{y}, \dot{\mathbf{y}}) = \mathbf{f} \tag{1}$$

where **M**, **C** and **K** are the deterministic n-dimensional mass, damping and stiffness matrices associated with the linear counterpart of the structure, **f**(t) is the vector of random external forces (assumed to be Gaussian in this paper) and **y**(t) gathers the displacements of the nodes of the structural model.

These are expected to be non-Gaussian processes due to the nonlinear forces $\mathbf{g}(\mathbf{y},\dot{\mathbf{y}})$.

Application of standard stochastic linearization techniques [4] provides the equivalent linearized equation of motion

$$\mathbf{M}\ddot{\mathbf{x}} + (\mathbf{C}+\mathbf{C}_{eq})\,\dot{\mathbf{x}} + (\mathbf{K}+\mathbf{K}_{eq})\,\mathbf{x} = \mathbf{f} \tag{2}$$

which is readily solved in a spectral analysis

$$\mathbf{S}_{\mathbf{x}} = \mathbf{H}_l \mathbf{S}_{\mathbf{f}} \mathbf{H}_l^* \tag{3}$$

where $\mathbf{S}_{\mathbf{x}}(\omega)$ and $\mathbf{S}_{\mathbf{f}}(\omega)$ represent the power spectral density matrices of the structural response and of the loading, while $\mathbf{H}_l(\omega)$ represents the n-dimensional frequency response function. It of course depends on $\mathbf{K}_{eq}$ and $\mathbf{C}_{eq}$, which is the central issue of this equivalence. Indeed matrices $\mathbf{K}_{eq}$ and $\mathbf{C}_{eq}$ represent the equivalent stiffness and damping matrices. They depend on the *a priori* unknown covariance matrix of nodal displacements and velocities $\boldsymbol{\Sigma}_{\mathbf{x}}$ and $\boldsymbol{\Sigma}_{\dot{\mathbf{x}}}$ expressed as

$$\boldsymbol{\Sigma}_{\mathbf{x}} = \int_{\mathbb{R}} \mathbf{S}_{\mathbf{x}} d\omega \tag{4}$$

$$\boldsymbol{\Sigma}_{\dot{\mathbf{x}}} = \int_{\mathbb{R}} \omega^2 \mathbf{S}_{\mathbf{x}} d\omega \tag{5}$$

The equivalent matrices and the covariance matrices are thus determined with an iterative scheme, as a result of the equivalence equations [1]

$$\mathbf{K}_{eq} = \boldsymbol{\Sigma}_{\mathbf{x}}^{-1} E\left[\mathbf{x}\mathbf{g}(\mathbf{x},\dot{\mathbf{x}})^T\right] \tag{6}$$

$$\mathbf{C}_{eq} = \boldsymbol{\Sigma}_{\dot{\mathbf{x}}}^{-1} E\left[\dot{\mathbf{x}}\mathbf{g}(\mathbf{x},\dot{\mathbf{x}})^T\right] \tag{7}$$

For most common types of nonlinearities $\mathbf{g}(\mathbf{y},\dot{\mathbf{y}})$, the expectations may be worked out in closed form so that (6)-(7) may be translated into the explicit form

$$\mathbf{K}_{eq} = \mathcal{K}\left(\boldsymbol{\Sigma}_{\mathbf{x}}, \boldsymbol{\Sigma}_{\dot{\mathbf{x}}}\right), \tag{8}$$

$$\mathbf{C}_{eq} = \mathcal{C}\left(\boldsymbol{\Sigma}_{\mathbf{x}}, \boldsymbol{\Sigma}_{\dot{\mathbf{x}}}\right). \tag{9}$$

Implementation of the fixed-point algorithm requires (i) to initiate $\mathbf{K}_{\mathbf{eq}}$ and $\mathbf{C}_{\mathbf{eq}}$ to a start-up value (usually zero), (ii) to provide a provisional estimation of the covariance matrices $\boldsymbol{\Sigma}_{\mathbf{x}}$ and $\boldsymbol{\Sigma}_{\dot{\mathbf{x}}}$ with (3)-(5), (iii) to update $\mathbf{K}_{eq}$ and $\mathbf{C}_{eq}$ with (8)-(9) and (iv) iterate until convergence is (hopefully) reached.

In order to bypass the computationally expensive construction and double multiplication of these matrices, reflexes of linear structural dynamics drives the solution (3) toward a reduced basis analysis. For a linear equation as (2), the modal basis is demonstrated to be optimum [7]. Some sort of optimality would thus request the use of the normal modes of vibration resulting from the eigenvalue problem

$$(\mathbf{K}+\mathbf{K}_{eq})\,\boldsymbol{\Phi}_{\boldsymbol{o}} = \omega^2 \mathbf{M}\boldsymbol{\Phi} \tag{10}$$

a solution that is immediately rejected as it would require the updating of the modal basis at each iteration, i.e. for every new value of $\mathbf{K}_{eq}$. Instead and inspired by a solution adopted in a similar context [8], we use a fixed modal basis defined as

$$\left(\mathbf{K}+\tilde{\mathbf{K}}\right)\boldsymbol{\Phi} = \omega^2 \mathbf{M}\boldsymbol{\Phi} \tag{11}$$

where $\tilde{\mathbf{K}}$ is there to represent the influence of the (*a priori* unknown) converged equivalent stiffness matrix, on the natural mode shapes and frequencies of the underlying linear problem, i.e. (1) without **g**.

Although we present it as a fixed estimation, one might desire to update the matrix $\tilde{\mathbf{K}}$ during the iterations of the solution algorithm, be it the fixed-point or not, in order to optimize this tuning. This option is open and should be used wisely in order not to lapse again in an eigenvalue decomposition at each step of the algorithm. Our experience has demonstrated that two to three updates in a moderately nonlinear problem is by far sufficient.

In this reduced basis where the generalized shapes are normalized through the mass matrix $\boldsymbol{\Phi}^T\mathbf{M}\boldsymbol{\Phi} = \mathbf{I}$, the governing equation (2) becomes

$$\ddot{\mathbf{q}} + (\mathbf{D}+\mathbf{D}_{eq})\,\dot{\mathbf{q}} + (\boldsymbol{\Omega}+\boldsymbol{\Omega}_{eq})\,\mathbf{q} = \mathbf{p} \tag{12}$$

where

$$\begin{aligned} \mathbf{D} &= \boldsymbol{\Phi}^T\mathbf{C}\boldsymbol{\Phi} \qquad & \mathbf{D}_{eq} &= \boldsymbol{\Phi}^T\mathbf{C}_{eq}\boldsymbol{\Phi} \\ \boldsymbol{\Omega} &= \boldsymbol{\Phi}^T\mathbf{K}\boldsymbol{\Phi} \qquad & \boldsymbol{\Omega}_{eq} &= \boldsymbol{\Phi}^T\mathbf{K}_{eq}\boldsymbol{\Phi} \end{aligned} \tag{13}$$

and where $\mathbf{p}(t) = \boldsymbol{\Phi}^T\mathbf{f}(t)$ represents the generalized forces.

Because the generalized basis is not the modal basis $\boldsymbol{\Phi}_{\boldsymbol{o}}$, the generalized stiffness matrix $\boldsymbol{\Omega}$ is not diagonal. Nor is the generalized damping matrix **D**. The generalized equivalent matrices $\boldsymbol{\Omega}_{eq}$ and $\mathbf{D}_{eq}$ are certainly not diagonal either. All in all, the projection into a reduced basis has limited the number of degrees-of-freedom to a bunch of modes (at the opposite of the large number of degrees-of-freedom of the nodal model (2), possibly), but has not uncoupled the equations of motion, as a formal modal basis would have produced.

The response in the generalized basis reads

$$\mathbf{S}_{\mathbf{q}} = \mathbf{H}\mathbf{S}_{\mathbf{p}}\mathbf{H}^* \tag{14}$$

where the psd matrix of the generalized forces is $\mathbf{S}_{\mathbf{p}} = \boldsymbol{\Phi}^T\mathbf{S}_{\mathbf{f}}\boldsymbol{\Phi}$ and the generalized frequency response function is $\mathbf{H} = \left(-\mathbf{I}\omega^2 + \mathrm{j}\omega\left(\mathbf{D}+\mathbf{D}_{eq}\right) + \left(\boldsymbol{\Omega}+\boldsymbol{\Omega}_{eq}\right)\right)^{-1}$. The covariance matrices of the generalized responses and velocities read

$$\boldsymbol{\Sigma}_{\mathbf{q}} = \int_{\mathbb{R}} \mathbf{S}_{\mathbf{q}} d\omega \tag{15}$$

$$\boldsymbol{\Sigma}_{\dot{\mathbf{q}}} = \int_{\mathbb{R}} \omega^2 \mathbf{S}_{\mathbf{q}} d\omega \tag{16}$$

In the reduced basis, implementation of the fixed-point method translates into (i) initiation of $\mathbf{K}_{eq}$ and $\mathbf{C}_{eq}$, (ii) setting up the provisional estimation of $\boldsymbol{\Sigma}_{\mathbf{x}}$ and $\boldsymbol{\Sigma}_{\dot{\mathbf{x}}}$ from (12-14) and

$$\boldsymbol{\Sigma}_{\mathbf{x}} = \boldsymbol{\Phi}\boldsymbol{\Sigma}_{\mathbf{q}}\boldsymbol{\Phi}^T \tag{17}$$

$$\boldsymbol{\Sigma}_{\dot{\mathbf{x}}} = \boldsymbol{\Phi}\boldsymbol{\Sigma}_{\dot{\mathbf{q}}}\boldsymbol{\Phi}^T \tag{18}$$

then (iii) to update $\mathbf{K}_{eq}$ and $\mathbf{C}_{eq}$ with (8)-(9) and (iv) iterate.

2.2 Second-order Algorithm

The fixed-point algorithm as exposed above is definitely convenient for practical purposes, but has unfortunately convergence properties that are known to be rather poor [9].

As an alternative we suggest to use a formal Newton-Raphson approach for the solution of the same set of equations.

Plugging (15)-(16) into (17)-(18) and further elaborating the expression of $\mathbf{S_q}$, from (14), where the dependence of $\mathbf{K}_{eq}$ and $\mathbf{C}_{eq}$ in $\mathbf{H}(\omega)$ is explicitly developed, yield, after finally considering (8)-(9),

$$\mathcal{R}\left(\left\{\begin{array}{c}\boldsymbol{\Sigma}_{\mathbf{x}}\\ \boldsymbol{\Sigma}_{\dot{\mathbf{x}}}\end{array}\right\}\right)=\left\{\begin{array}{c}\boldsymbol{\Sigma}_{\mathbf{x}}\\ \boldsymbol{\Sigma}_{\dot{\mathbf{x}}}\end{array}\right\}+\mathcal{F}\left(\left\{\begin{array}{c}\boldsymbol{\Sigma}_{\mathbf{x}}\\ \boldsymbol{\Sigma}_{\dot{\mathbf{x}}}\end{array}\right\}\right)=0 \tag{19}$$

where the first term of the residue $\mathcal{R}$ originates from the lefthand sides of (17)-(18), while operator $\mathcal{F}$ is an assemblage of matrix multiplications and integrations on the frequency space, as per its construction described above.

This operation has reset the problem into a usual format that is suitable for a Newton-Raphson solution. Writing $\boldsymbol{\sigma}=\{\boldsymbol{\Sigma}_{\mathbf{x}};\boldsymbol{\Sigma}_{\dot{\mathbf{x}}}\}$, the *(n+1)th* iterate is obtained as

$$\boldsymbol{\sigma}_{n+1}=\boldsymbol{\sigma}_n-\mathbf{J}_n\mathcal{R}\left(\boldsymbol{\sigma}_n\right) \tag{20}$$

starting from the response of the underlying linear system (setting **g** to zero) as an initial estimate, and where

$$\mathbf{J}_n=\mathbf{J}\left[\boldsymbol{\sigma}_n\right]=\nabla_{\boldsymbol{\sigma}}\mathcal{R}^{\mathrm{T}}=\mathbf{I}-\nabla_{\boldsymbol{\sigma}}\mathcal{F}^{\mathrm{T}} \tag{21}$$

represents the Jacobian of the residual function $\mathcal{R}$. These equations demonstrate that the implementation of a second-order accurate numerical method is possible. In practice, the implementation of this technique is not necessarily auspicious as the derivatives taking place in the expression of the Jacobian would be performed with a finite difference approximation. This operation requires a tremendous number of operations, as derivatives have to be established for each degree-of-freedom (in position and velocity).
With the following approach, we propose however a rapid and accurate way to solve this issue, and therefore to keep on working with a Newton-Raphson algorithm.

2.3 Non-diagonal modal matrices

The governing equations in the generalized basis (12) are slightly to moderately coupled, depending on the intensity of the nonlinear forces in the global balance of forces, as a result of the projection into a fixed basis. The origin of the drift is threefold. First, the larger the nonlinear forces, the more different the generalized basis from the modal basis, which results in a coupled generalized stiffness matrix. Second, the same argument holds for the damping matrix, which is however also complemented by a modal diagonality assumption, such as in the Rayleigh damping. Third, the larger the nonlinear forces, the larger $\boldsymbol{\Omega}_{eq}$ and $\mathbf{D}_{eq}$ compared to $\boldsymbol{\Omega}$ and $\mathbf{D}$.

Former works have demonstrated the advantage of considering this kind of coupled set of modal equations as a perturbation of the uncoupled problem [5,6]. To this aim, the generalized damping and stiffness matrices are split into two contributions each

$$\mathbf{D}+\mathbf{D}_{eq}:=\mathbf{D}_d+\mathbf{D}_o \qquad \boldsymbol{\Omega}+\boldsymbol{\Omega}_{eq}:=\boldsymbol{\Omega}_d+\boldsymbol{\Omega}_o \tag{22}$$

such that the generalized frequency response function **H** reads

$$\mathbf{H}=\left(\mathbf{G}_d+\mathbf{G}_o\right)^{-1} \tag{23}$$

with

$$\mathbf{G}_d=\boldsymbol{\Omega}_d-\omega^2\mathbf{I}+\iota\omega\mathbf{D}_d, \qquad \mathbf{G}_o=\boldsymbol{\Omega}_o+\iota\omega\mathbf{D}_o \tag{24}$$

Under some smallness properties of the off-diagonal terms in (23), compared to the diagonal ones –which is formally expressed by $\boldsymbol{\rho_J}<1$, i.e. the spectral radius $\boldsymbol{\rho_J}$ of $\mathbf{G}_d^{-1}\mathbf{G}_o$, where we also notice that $\mathbf{H}_d=\mathbf{G}_d^{-1}$ corresponds to the frequency response function that would be obtained it there were no off-diagonal terms–, a convergent series expansion of **H** reads

$$\mathbf{H}=\left(\mathbf{I}+\sum_{i=1}^{\infty}\left(-\mathbf{G}_d^{-1}\mathbf{G}_o\right)^i\right)\mathbf{H}_d \tag{25}$$

so that the generalized response (14) translates into

$$\mathbf{S}_{\mathbf{q}}=\left(\mathbf{I}+\sum_{i=1}^{\infty}\left(-\mathbf{H}_d\mathbf{G}_o\right)^i\right)\mathbf{S}_{\mathbf{q}_d}\left(\mathbf{I}+\sum_{j=1}^{\infty}\left(-\mathbf{G}_o^*\mathbf{H}_d^*\right)^j\right) \tag{26}$$

or, after expanding and collecting both series, then truncating the result to *N* terms,

$$\mathbf{S}_{\mathbf{q},N}=\mathbf{S}_{\mathbf{q}_d}+\sum_{k=1}^{N}\Delta\mathbf{S}_{\mathbf{q},k} \tag{27}$$

The response is thus seen as a perturbation of the response $\mathbf{S}_{\mathbf{q}_d}$ that would be obtained if the off-diagonal coupling terms were all neglected.

The format of this equation is particularly efficient in an implementation stage as it does not involve any matrix inversion, contrary to the formulation based on the formal expression (14). Indeed, expanding out the algebra from (26) to (27), the successive correction terms are shown to be given by

$$\Delta\mathbf{S}_{\mathbf{q},1}(\omega)=-\mathbf{H}_d\mathbf{G}_o\mathbf{S}_{\mathbf{q}_d}-\mathbf{S}_{\mathbf{q}_d}\mathbf{G}_o^*\mathbf{H}_d^* \tag{28}$$

and the following recurrence for *k* larger than 1,

$$\begin{aligned}\Delta\mathbf{S}_{\mathbf{q},k}(\omega)=&-\left(\mathbf{H}_d\mathbf{G}_o\Delta\mathbf{S}_{\mathbf{q},k-1}+\Delta\mathbf{S}_{\mathbf{q},k-1}\mathbf{G}_o^*\mathbf{H}_d^*\right)\\&-\mathbf{H}_d\mathbf{G}_o\Delta\mathbf{S}_{\mathbf{q},k-2}\mathbf{G}_o^*\mathbf{H}_d^*\end{aligned} \tag{29}$$

In these two relations, the only matrix inversion concerns the establishment of $\mathbf{H}_d$, which is trivial and inexpensive for it is diagonal.

Keeping everything unchanged in the estimation of the residual (19), but the estimation of $\mathbf{S_q}$ with an *N*-order truncated approximation (26) instead of the formal ($N=\infty$) approach (14), we thus provide a much faster estimation of the residual $\mathcal{R}$. This in turn brings significant saving on the solution algorithm, since the residual has to be estimated once at each iteration (in the fixed-point formulation). The saving is even more appreciated when the solution is performed with the Newton-Raphson algorithm as, in the basic formulation exposed earlier, each entry of the Jacobian requires another estimation of the residual (except that symmetry could interestingly invoked) for its finite difference estimation.

It is well known that an inexact estimation of the Jacobian worsens the convergence order of the Newton-Raphson [9].

What only matters to preserve the convergence of the algorithm is a proper estimation of the residual. Of course, the convergence rate worsens according to the severity of the approximation of the Jacobian. The better the estimation, the higher the convergence rate.

Even with the asymptotic expansion (27), the analytical expression of the residual remains rather heavy. Indeed with the explicit expression of operator $\mathcal{F}$, we have

$$\mathcal{R}_1 = \boldsymbol{\Sigma}_{\mathbf{x}} - \boldsymbol{\Phi}\left(\int_{\mathbb{R}}\left(\mathbf{S}_{\mathbf{q}_d} + \sum_{k=1}^{N}\Delta\mathbf{S}_{\mathbf{q},k}\right)d\omega\right)\boldsymbol{\Phi}^T \tag{30}$$

$$\mathcal{R}_2 = \boldsymbol{\Sigma}_{\dot{\mathbf{x}}} - \boldsymbol{\Phi}\left(\int_{\mathbb{R}}\omega^2\left(\mathbf{S}_{\mathbf{q}_d} + \sum_{k=1}^{N}\Delta\mathbf{S}_{\mathbf{q},k}\right)d\omega\right)\boldsymbol{\Phi}^T \tag{31}$$

where $\mathbf{S}_{\mathbf{q}_d}$ as well as $\Delta\mathbf{S}_{\mathbf{q},k}$ are both functions of the unknown covariance matrices $\boldsymbol{\Sigma}_{\mathbf{x}}$ and $\boldsymbol{\Sigma}_{\dot{\mathbf{x}}}$, through $\mathbf{H}$, which itself depends on $\mathbf{K}_{eq}$ and $\mathbf{C}_{eq}$ after (8)-(9). The derivatives of these components of the residual function, with respect to $\boldsymbol{\Sigma}_{\mathbf{x}}$ and $\boldsymbol{\Sigma}_{\dot{\mathbf{x}}}$ lead to endless chain rule differentiations and provide a too complex result.

Instead, driven by the idea of the dishonest Newton-Raphson, it is possible to provide an approximation of the Jacobian of the problem. It is developed in two steps. First we observe that the integrand inside the brackets in (30) is nothing but the power spectral density of the generalized coordinates $\mathbf{S}_{\mathbf{q}}$. Avoiding the series expansion in this first step, the derivative of $\mathbf{S}_{\mathbf{q}}$ with respect to $\boldsymbol{\sigma}$ reads

$$\nabla_{\boldsymbol{\sigma}}\left(\int_{\mathbb{R}}\mathbf{H}\mathbf{S}_{\mathbf{p}}\mathbf{H}^*d\omega\right) = \int_{\mathbb{R}}\left(\nabla_{\boldsymbol{\sigma}}\mathbf{H}\right)\mathbf{S}_{\mathbf{p}}\mathbf{H}^*d\omega + \int_{\mathbb{R}}\mathbf{H}\mathbf{S}_{\mathbf{p}}\left(\nabla_{\boldsymbol{\sigma}}\mathbf{H}^*\right)d\omega \tag{32}$$

with no assumption. The central issue with the endless chain rule differentiation pertains to the factor $\nabla_{\boldsymbol{\sigma}}\mathbf{H}$. In a second step, with two approximations related to the series expansion of the generalized frequency response function (25), we write

$$\begin{aligned}\nabla_{\boldsymbol{\sigma}}\mathbf{H} &\simeq \nabla_{\boldsymbol{\sigma}}\left(\left(\mathbf{I} - \mathbf{H}_d\mathbf{G}_o\right)\mathbf{H}_d\right)\\ &\simeq -\mathbf{H}_d\left(\nabla_{\boldsymbol{\sigma}}\boldsymbol{\Omega}_{eq} + \mathrm{j}\omega\nabla_{\boldsymbol{\sigma}}\mathbf{D}_{eq}\right)\mathbf{H}_d\end{aligned} \tag{33}$$

where the first approximation consists in trunctating the series (25) after the first term, while the second approximation limits the chain rule differentiation.

Considering the definitions in (13), the two remaining derivatives in (33), namely $\nabla_{\boldsymbol{\sigma}}\boldsymbol{\Omega}_{eq}$ and $\nabla_{\boldsymbol{\sigma}}\mathbf{D}_{eq}$, are readily expressed as a function of the derivatives of $\mathcal{K}$ and $\mathcal{C}$. This straightforwardness only holds because of our specific choice to work with a constant reduced basis $\boldsymbol{\Phi}$.

To summarize, the asymptotic expansion (25) has brought an efficient way to determine the residual function, as well as an approximation of the Jacobian of the problem, which opens the door to application of a dishonest Newton-Raphson procedure. Some additional algorithmic benefits of the formulation are detailed in [10].

3 ILLUSTRATIONS

A multistory shear-type building under a uni-dimensional seismic excitation is considered. The structural model consists of N_s=10 stories modeled by lumped masses m connected by geometrically nonlinear beam elements. The hardening behavior of steel beams is taken into account for large elastic displacements by an additional cubic nonlinear stiffness as in [11,12]. The structure is sketched in Fig. 1 and the equation of motion for the j^{th} story is

$$\begin{aligned}m\ddot{Y}_j + c\dot{Y}_j + k\left(Y_{j+1} - 2Y_j + Y_{j-1}\right)\\ + g_j(Y_{j-1}, Y_j, Y_{j+1}) = -m\ddot{U}\end{aligned} \tag{34}$$

where g_j is the j^{th} component of the nonlinear force vector with $1 \leq j \leq N_s-1$, defined as

$$\begin{aligned}g_j(Y_{j-1}, Y_j, Y_{j+1})\\ = \varepsilon k\left(\left(Y_j - Y_{j-1}\right)^3 - \left(Y_{j+1} - Y_j\right)^3\right)\end{aligned} \tag{35}$$

and where Y_j represents the horizontal displacement of storey j with respect to the ground motion. The structural masses and stiffnesses are m=1290tons, k=10^8 N/m and c results from a Rayleigh damping imposed to 1% in the first two linear modes. The natural frequencies of the first five linear normal modes are 0.21, 0.62, 1.02, 1.40, 1.75Hz.

The parameter ε quantifies the intensity of the nonlinear forces. It is considered as a variable parameter in this example in order to demonstrate the viability of the proposed approach for slightly to moderately nonlinear structures.

The 1-D ground motion is modeled with a modified Kanai-Tajimi spectrum [3], with the stationary power spectral density given as

$$S_{\ddot{U}} = S_0\frac{\left(1 + 4\xi_1^2\left(\frac{\omega}{\omega_1}\right)^2\right)}{\left(1 - \left(\frac{\omega}{\omega_1}\right)^2\right)^2 + 4\xi_1^2\left(\frac{\omega}{\omega_1}\right)^2}\frac{\left(\frac{\omega}{\omega_2}\right)^4}{\left(1 - \left(\frac{\omega}{\omega_2}\right)^2\right)^2 + 4\xi_2^2\left(\frac{\omega}{\omega_2}\right)^2} \tag{36}$$

with ω_1=5rad/s, ξ_1=0.2, ω_2=0.5rad/s, ξ_2=0.6 and S_0=0.03 m²/s³.

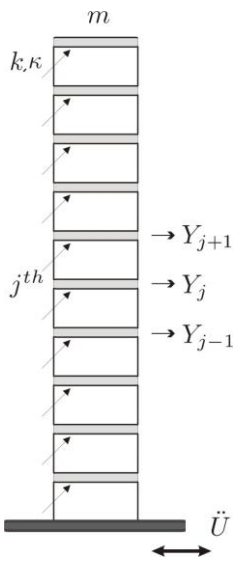

Figure 1. Sketch of the considered structure.

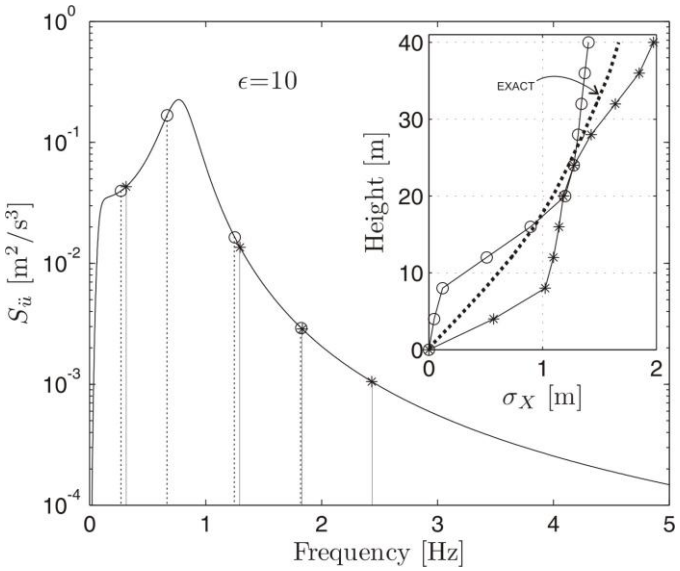

Figure 2. Illustration of the lack of convergence of the fixed-point algorithm. The main graph represents the power spectral density of the ground excitation; the vertical lines localize the natural frequencies of two successive iterates (shown in inset).

The classical fixed-point method fails to converge in the solution of this problem for moderate nonlinear behavior. The algorithm is trapped in a period-2 cycling, without converging thus. This is illustrated in Fig. 2 with results obtained in the nodal basis for the 10 degrees-of-freedom. After a number of iterations, the algorithm provides a provisional estimation of the covariance matrix $\mathbf{\Sigma_x}$ that is large enough (result with stars in Fig. 2) to provide a significant equivalent stiffness matrix $\mathbf{K}_{eq}$, compared to the initial stiffness matrix of the underlying linear model. This additional damping substantially shifts up the natural frequencies of the equivalent linearized structure. This increase in the natural frequencies translates into a reduction of the response, since the frequency content of the ground excitation is smaller at high frequency. Consequently, the new iterate of the covariance matrix $\mathbf{\Sigma_x}$ is much smaller than the former provisional state. This leads to a smaller equivalent stiffness matrix and finally larger ground excitation which drive the iterations back again to the provisional state. Figure 2 illustrates this lack of convergence of the fixed-point algorithm. The inset shows the covariance of nodal displacements corresponding to these two iterates between which the algorithm switches back and forth. The exact solution lies somewhere in-between, as indicated by the thick dashed line.

For value of ε smaller than 10 (the numerical value considered in Fig. 2), the convergence of the fixed-point algorithm is actually really slow, for similar reasons.

The explanations given above make it clear that this poor convergence is a result of the decreasing nature of the power spectral density of the excitation. A reason why this sort of lack of convergence is seldom illustrated is that the typically considered academic examples assumed a white noise or broad band, ground excitation. This prohibits the occurrence of the period-2 cycling in the algorithm performances.

For this problem, the proposed method (with N=2, two terms in the series expansion) reaches convergence thanks to the advanced convergence properties of the Newton-Raphson algorithm. We also take advantage of this example to illustrate the updating procedure of the equivalent matrix $\tilde{\mathbf{K}}$ that is used to determine the reduced basis.

In a first run, the linear structure (ε=0) is analyzed. This provides a first estimation of the covariance matrices of displacements and velocities. To compute the equivalent matrix $\tilde{\mathbf{K}}$ with the response of the linear system proves to be too severe. Instead, only a fraction of the variances of the displacements and velocities of the linear structure are considered. Consistently with the ratio the internal forces from the linear structure and those in the equivalent linear one, this fraction is chosen as $1/(1+3\varepsilon)$. In the sequel, we explore the possibility to update the equivalent matrix $\tilde{\mathbf{K}}$ until twice during the iterations of the Newton-Raphson algorithm. Update is to be activated when the convergence criterion of the asymptotic series (25) is weak, or when getting closer to the converged solution. In this latter case, an ultimate update of the equivalent matrix $\tilde{\mathbf{K}}$ offers a more accurate reduced basis, and therefore a more accurate estimation of the structural response $\mathbf{\Sigma_x}$ and $\mathbf{\Sigma_{\dot{x}}}$.

In all simulations, five modes are kept in the reduced basis. Although the index of off-diagonality ρ_J is rather large when the equivalent stiffness matrix is not updated, see results labelled $\tilde{\mathbf{K}}^{(0)}$ in Fig. 4-a, this actually does not prevent the proposed method to converge. However, there remains a discrepancy with the exact solution because the approximation of the equivalent stiffness matrix does not exactly fit the equivalent stiffness matrix corresponding to the final displacement. With this respect, the projection into five mode shapes is not rich enough to represent the covariance of the response.

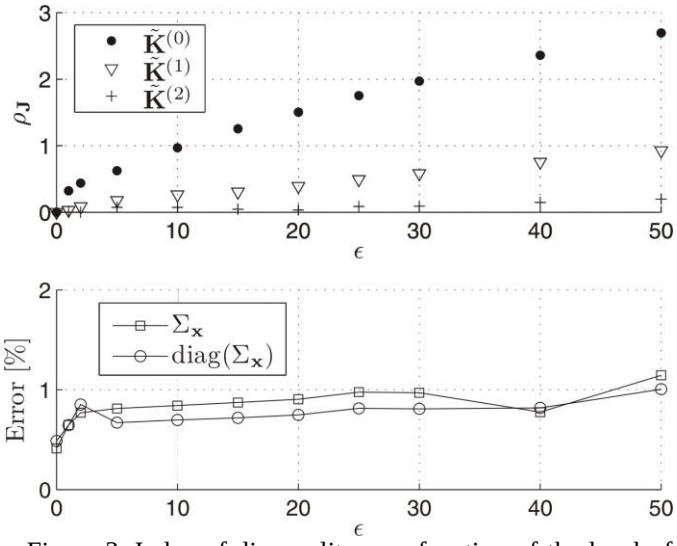

Figure 3. Index of diagonality as a function of the level of nonlinearity and error estimates on the covariance of the response (estimated with respect to the exact linearization).

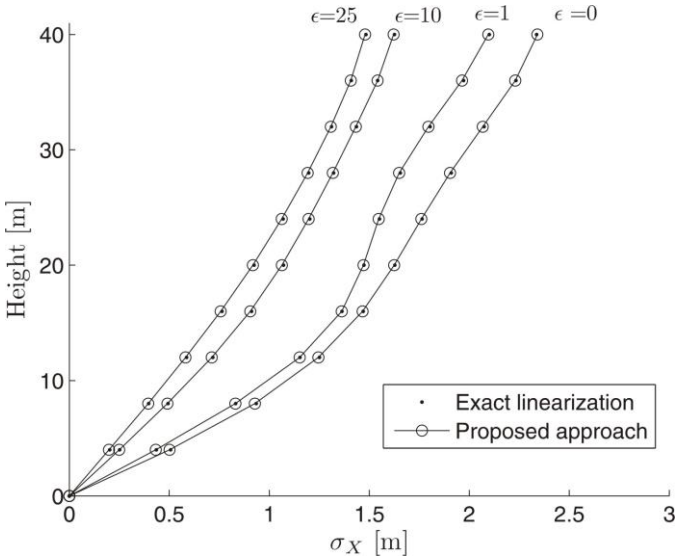

Figure 4. Standard deviation of the transverse displacement for various level of the nonlinearity. The proposed approach matches perfectly the results of the exact linearization.

However, with one, respectively two, update(s) of the equivalent stiffness matrix, as represented by the results labelled $\tilde{\mathbf{K}}^{(1)}$ and $\tilde{\mathbf{K}}^{(2)}$ in Fig. 4-a, these two limitations are circumvented at once. On the one hand, we can decrease the diagonality index to very small values, which ensures the fast convergence of the series expansion (25). This guarantees a perfect accuracy of the second order approximation (N=2) of the series. On the other hand, with an update or two of the equivalent stiffness matrix, the reduced basis in which the response is projected much better suit the formal normal modes of vibration of the equivalent linear system, as given in (10).

The proposed approach was tested for several values of the parameter ε, which rules the intensity of the nonlinear forces. Every result displayed in Figs 3-4 is obtained from a condition at rest, and thus not on with a continuation procedure. This just aims at demonstrating that our algorithmic arrangement is able to cope with initial conditions that are possibly large from the actual solution.

With the initial estimation of $\tilde{\mathbf{K}}$, convergence toward a solution is achieved with less than four iterations, in any configuration (ε in [0;50]). In order to illustrate the influence of the update of the equivalent stiffness matrix $\tilde{\mathbf{K}}$, its is updated once from this converged solution. Another series of iterations (four again at most) provides a better estimation of the covariance of the nodal displacement. At last but not least, whenever a second update of $\tilde{\mathbf{K}}$ is required, we extend with a couple of iterations, from there again, with the updated matrix.

This finally provides the results of Fig. 4, which are virtually in perfect agreement with the results obtained with a formal solution of the equivalent stochastic linearization procedure. This latter reference results were obtained with the fixed-point method, started this time from the converged solution of our algorithm. As is starts close enough to the exact solution, the fixed-point method behaves much better in this case. The results in Fig. 4 indicate that ε =25 produced significant nonlinear forces, as it results in a decrease of the response of the linear system (ε =0) by almost 50%.

The overall 2-norm error, reported in Fig 3-a, is at most equal to 1%, both on the diagonal terms of the covariance as well as on the whole covariance matrix itself. This observation is also valid for large nonlinearities, as the only remaining assumption in the method is related to the truncation of the series expansion, which after all converges very fast as the diagonality index is kept very small.

4 CONCLUSIONS

The proposed developments demonstrate that for slightly coupled nonlinear systems, the equivalent linearization can be seen as a convergent series of correction terms around the stochastic response of a main decoupled linearized system. The computational effort is thus attractively reduced, while the method also offers much insight on how to physically interpret the nonlinear coupling.

The concept of asymptotic expansion of modal transfer matrix can thus be used to speed up the solution of the large equation set involving integrals by avoiding inversion of full transfer matrices and repeated integrations.

ACKNOWLEDGMENTS

TC acknowledges the support of the FNRS (Fond National de la Recherche Scientifique).

REFERENCES

[1] Grigoriu, M., Stochastic calculus: applications in science and engineering. 2002: Springer Verlag, Birkhäuser. 774 p..

[2] Preumont, A., *Random Vibration and Spectral Analysis*, ed. K.A. Publishers. 1994: Kluwer Academic Publishers. 288 p.

[3] Clough, R.W. and J. Penzien, *Dynamics of structures*. 2nd edition ed, ed. McGraw-Hill. 1993, New-York: McGraw-Hill. 738 p.

[4] Roberts, J.B. and P.D. Spanos, *Random Vibration and Statistical Linearization*, ed. J.W. Sons. 1999: Dover Publications.

[5] Denoël, V. and H. Degée, *Asymptotic expansion of slightly coupled modal dynamic transfer functions.* Journal of Sound and Vibration, 2009. **328**(1-2): pp. 1-8.

[6] Canor, T., N. Blaise, and V. Denoël, *Efficient uncoupled stochastic analysis with non-proportional damping.* Journal Of Sound And Vibration, 2012. **331**(24): pp. 5283-5291.

[7] Géradin, M. and D. Rixen, Mechanical vibrations: theory and application to structural dynamics, ed. Lavoisier. 2002. 500 p.

[8] Proppe, C., H.J. Pradlwarter, and G.I. Schueller, *Equivalent linearization and Monte Carlo simulation in stochastic dynamics.* Probabilistic Engineering Mechanics, 2003. **18**(1): pp. 1-15.

[9] Quarteroni, A., R. Sacco, and F. Saleri, *Numerical Mathematics*. 2nd Edition ed. Texts in Applied Mathematics. Vol. 1. 2007, Berlin: Springer Verlag. 610p.

[10] Canor, T., N. Blaise, and V. Denoël, An asymptotic expansion method in equivalent statistical linearization, submitted to Probabilistic Engineering Mechanics.

[11] Lin, Y.K. and G.Q. Cai, Probabilistic Structural Dynamics: Advanced Theory and Applications. 2004: McGraw-Hill.

[12] G. Ricciardi. A non-Gaussian stochastic linearization method. Probabilistic Engineering Mechanics, 22(1):1–11, 2007.